Pergamon

Int. J. Mach. Tools Manufact. Vol. 37, No. 7, pp. 947–967, 1997

Printed in Great Britain
0890-6955/97$17.00 + .00

PII: S0890-6955(96)00088-0

# CROSS-COUPLED PRECOMPENSATION METHOD FOR THE CONTOURING ACCURACY OF COMPUTER NUMERICALLY CONTROLLED MACHINE TOOLS

JIH-HUA CHIN†‡ and TSUNG-CHING LIN†

(*Received* 21 *July* 1995; *in final form* 16 *September* 1996)

**Abstract**—A cross-coupled precompensation method (CCPM) for precise trajectories of machine tools is proposed in this study. Compared with the conventional cross-coupled system and uncoupled system by computer simulation and experiment, the pure precompensation method is better in dealing with the circular trajectory and the elimination of the steady-state errors, while the CCPM can achieve the most precise tracking for both linear and circular trajectory at any feedrate. The advantages of CCPM will be enhanced at higher feedrates. At a feedrate of 200 mm/sec the CCPM stands out significantly. © 1997 Elsevier Science Ltd. All rights reserved

## NOMENCLATURE

| | |
|---|---|
| $x,y$ | the index for $X,Y$-axis |
| $K_c$ | digital-to-analog gain in vol./bit |
| $K = K_m K_c$ | partial loop gain |
| $K_m$ | axial drive gain |
| $K_c$ | encoder gain |
| $\tau$ | time constant |
| $V_d$ | feedrate |
| $K_v$ | precompensated gain |
| $K_{ex}, K_{ey}$ | gains of contour error compensation in $X,Y$-axis |
| $K_{ex}, K_{ey}$ | gains of tracking error compensation in $X,Y$-axis |
| US | uncoupled system |
| CCS | cross-coupled control system |
| PM | precompensation method |
| CCPM | cross-coupled precompensation method |
| IAE | integral absolute error |
| ITAE | integral-of-time multiplied absolute error |
| $\lvert\epsilon_{max}\rvert$ | absolute value of maximum contour error |
| SSE | steady-state error |
| $\phi$ | inclination of desired contour to $x$-axis |
| DDA | digital differential analyzer |
| DAC | digital-to-analog converter |
| $R$ | radial contour error |
| $R_i$ | actual radius |
| $T$ | sampling time interval |
| $V_{bx}, V_{by}$ | components of feedrate $V_b$ in the $X,Y$ coordinate |
| $V_{kx}, V_{ky}$ | components of connection velocity $V_k$ in the $X,Y$ coordinate |
| $\epsilon$ | contour error |
| $e$ | position errors |
| $V_b$ | command feeding velocity |
| $U$ | DAC input signal |
| $D$ | disturbance |

†Department of Mechanical Engineering, National Chiao Tung University, Hsinchu, Taiwan, Republic of China
‡To whom correspondence should be addressed.

## 1. INTRODUCTION

In a computer numerically controlled (CNC) machine tool, the cross-coupled control system (CCS) was designed to improve the contouring accuracy of specified trajectories rather than tracking their accuracy for precision machining. The term "contour accuracy" denotes the error component orthogonal to the desired trajectory, while the "tracking accuracy" is the error along the desired trajectory. The basic concept of a conventional CCS can be described in a block diagram (Fig. 1). This control system contributes to machining accuracy, particularly those linear trajectory accuracies of high speed continuous feed drivers, by developing contour error compensators. There exist a number of researches which have proved the obvious improvement of contouring accuracy obtained by adjusting the ratio $K_{ex}/K_{ex}$ or $K_{ey}/K_{ey}$ of a biaxial machine tool feed drive.

The first CCS, proposed by Sarachik and Ragazzini [1], was a "master–slave" and non-symmetrical structure. Koren and Ben-Uri [2, 3] proposed a symmetrical structure to improve the limitations of a non-symmetrical CCS, such as open-contour operations and steady-state contour error caused by the gain difference between axes. The mathematical analysis as well as the comparison with the conventional CNC system with individual axis control were provided.

Furthermore, the high feedrate varying from 37.5 mm/sec to 120 mm/sec in a cross-coupled system was discussed by Srinivasan and Kulkarni [4]. Later, Koren and Lo [5] proposed a variable gain cross-coupled controller for contours such as circles and parabolas. In recent years, Chuang and Liu proposed an adaptive feedrate control and model-referenced adaptive control strategy [6, 7]. An application of cross-coupled control in a retrofitted milling machine was proposed by Huang and Chen [8]. A path algorithm, named the path precompensation (PM) method, to pre-adapt the path parameters before tracking was presented by Chin and Tsai [9].

The main purpose of this paper is to propose a "cross-coupled PM" (CCPM) to improve the accuracy and to eliminate the steady-state error of the linear contour. The PM algorithm for the multi-axis machine tool in Cartesian space was used as a comparison base. The high speed cases, varying from 11.8 to 200 mm/sec, are also studied for the pure path PM and CCPM.

## 2. CROSS-COUPLED PRECOMPENSATION METHOD

In this section, we modify the path algorithm [9, 10] to pre-adapt the path parameters for tracking velocity regulation in Cartesian space and proceed to propose a control strategy for the CCPM which intends to combine the advantages of the path PM and conventional CCS.

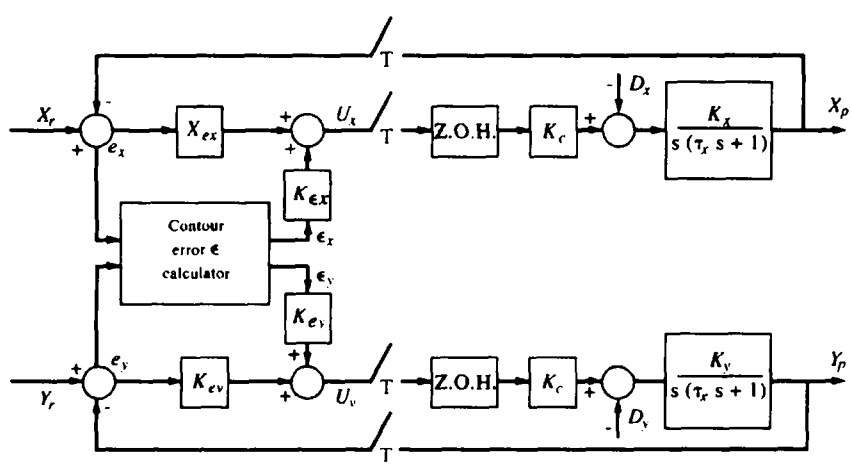


Fig. 1. Block diagram of conventional CCS.

2.1. *Path precompensation method*

2.1.1. *For a straight line.* A straight line shown in Fig. 2 lies, for example, in the first quadrant and the machine tool is feeding from point $P_a$ to point $P_e$ with a feed speed $V_b$. The contour error $\epsilon$ is defined as the least vertical distance between the actual position $P_i(x_i,y_i)$ and the straight line segment $\overline{P_aP_e}$,

$$\epsilon = x_i \sin \phi - y_i \cos \phi.$$

A velocity correction term $\vec{V}_k$ is defined toward $\overline{P_aP_e}$ with $V_k = K_v\epsilon$, where $K_v$ is a precompensating gain value to compensate the contour error.

By the combination of $V_b$ and $V_k$, two desired path velocity components about the $X$- and $Y$-axis, respectively, are obtained:

$$V_x = V_{bx} + V_{kx} = V_b \cos \phi - K_v\epsilon \sin \phi$$

$$V_y = V_{by} + V_{ky} = V_b \sin \phi + K_v\epsilon \cos \phi$$

where $X_{bx}$ and $V_{by}$ are components of feedrate $V_b$ in the $X,Y$-coordinate and $V_{kx}$ and $V_{ky}$ are components of correction velocity $V_k$ in the $X,Y$-coordinate.

2.1.2. *For a circular arc.* A circular arc path is shown in Fig. 3: the magnitude $R$ is the desired radius and $R_i$ is the actual radius. The contour error $\epsilon$ can be calculated as

$$\epsilon = R - R_i = R - (x_i^2 + y_i^2)^{\frac{1}{2}}.$$

In a similar way, the modified path velocity about the $X$- and $Y$-axes are obtained as

$$V_x = V_{bx} + V_{kx} = -V_b(y_i/R_i) + K_v\epsilon(x_i/R_i)$$

$$V_y = V_{by} + V_{ky} = V_b(x_i/R_i) + K_v\epsilon(y_i/R_i).$$

2.2. *The strategies of the cross-coupled precompensation method*

The proposed structure of a system with CCPM is shown in Fig. 4. Note that if the control gains $K_{ex}$ and $K_{ey}$ are set to zero, the system reduces to that with the path PM. However, the tracking mechanism, i.e. $K_{ex}$ and $K_{ey}$, is included which makes the PM strategy in this paper different from that described in [9, 10].

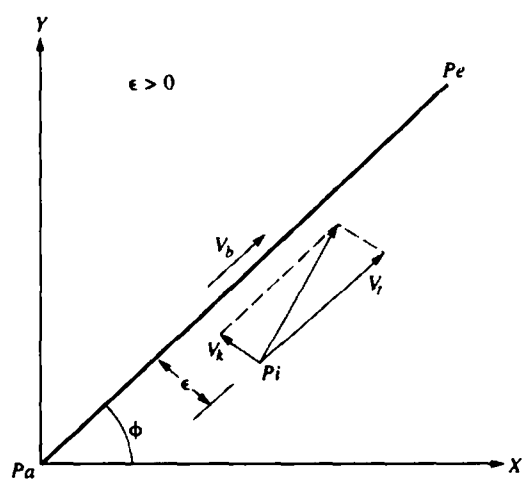


Fig. 2. Straight line regulation.

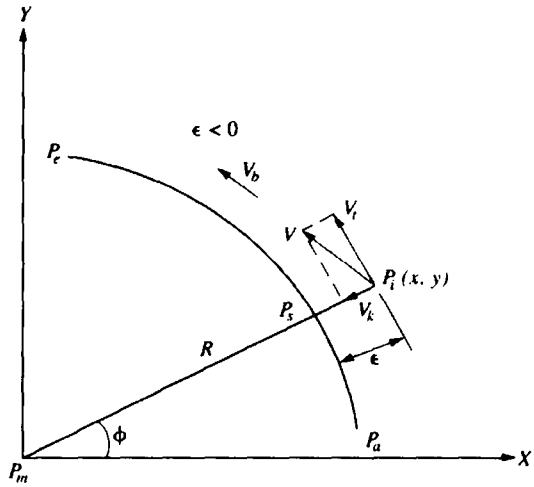


Fig. 3. Circular path regulation.

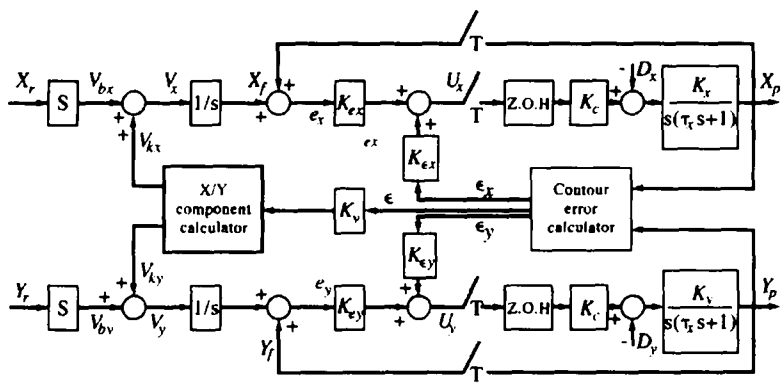


Fig. 4. Block diagram of cross-coupled precompensation system.

In the previous section, we represent the adjusted velocity $V_x, V_y$ as

$$V_x(n) = V_b \cos \phi - K_v \epsilon(n) \sin \phi$$

$$V_y(n) = V_b \sin \phi + K_v \epsilon(n) \cos \phi.$$

A new reference position $x_f, y_f$ is obtained by integrating $V_x, V_y$, the discrete form of which is

$$x_f(n) = x_f(n-1) + TV_x$$

$$y_f(n) = y_f(n-1) + TV_y$$

where $T$ is the sampling time interval.

Next, the feed position error can be determined by

$$e_x(n) = e_x(n-1) + x_f(n) - x_p(n)$$

$$e_y(n) = e_y(n-1) + y_f(n) - y_p(n)$$

and, the control signal $U_x, U_y$ is calculated from

$$U_x(n+1) = K_{ex}e_x(n) + K_{\epsilon x}\epsilon_x(n)$$

$$U_y(n+1) = K_{ey}e_y(n) + K_{\epsilon y}\epsilon_y(n).$$

There are different formulas for contour error calculations along different trajectories. In this study, the contour error $\epsilon$ on the linear contour can be determined as:

$$\epsilon(n) = x_p(n)\sin\phi - y_p(n)\cos\phi$$

and

$$\epsilon_x(n) = -\epsilon(n)\sin\phi$$

$$\epsilon_y(n) = \epsilon(n)\cos\phi.$$

On the circular contour, the contour error $\epsilon$ can be determined by

$$\epsilon(n) = R - (x_p(n)^2 - y_p(n)^2)^{1/2}$$

and

$$\epsilon_x(n) = \epsilon(n) \times \left(\frac{x_p(n)}{R_p(n)}\right)$$

$$\epsilon_y(n) = \epsilon(n) \times \left(\frac{y_p(n)}{R_p(n)}\right).$$

### 2.3. *Simulation studies*

For the sake of comparison with systems studied in [3, 5], the following parameters were adopted for computer simulations of linear and circular contours: $K_cK_x = 10.3$, $K_cK_y = 10.0$, $\tau_x = 0.04$, $V_b = 11.8$ mm/sec (28 in/min) and $|D_x| = |D_y| = 0.75$ . The resolution of position reading is 1 $\mu$m.

2.3.1. *Simulation results for linear contour.* Since optimization is not the purpose of this study, a group of gains $K_v$,$K_{\epsilon x}$,$K_{\epsilon y}$,$K_{ex}$ and $K_{ey}$ which give the smallest contour errors for the respective methods were chosen and compared in Tables 1 and 2 for a linear contour at an angle $\phi = 45°$ (see Fig. 5).

Table 1. Gains used for four control schemes for a linear contour

| | $K_v$ | $K_{\epsilon x}$ | $K_{\epsilon y}$ | $K_{ex}$ | $K_{ey}$ |
|---|---|---|---|---|---|
| US | 0 | 0 | 0 | 12 | 12 |
| CCS | 0 | 15 | 15 | 0.5 | 0.5 |
| PM | 8 | 0 | 0 | 3.5 | 3.5 |
| CCPM | 13 | 15 | 15 | 0.5 | 0.5 |

Table 2. Simulation results corresponding to Table 1

| | Fig. 5 | $\lvert\epsilon_{max}\rvert$ ($\mu$m) | SSE ($\mu$m) |
|---|---|---|---|
| US | (a) | 25 | 3 |
| CCS | (b) | 2.5 | 1 |
| PM | (c) | 23 | 0 |
| CCPM | (d) | 2.5 | 0 |

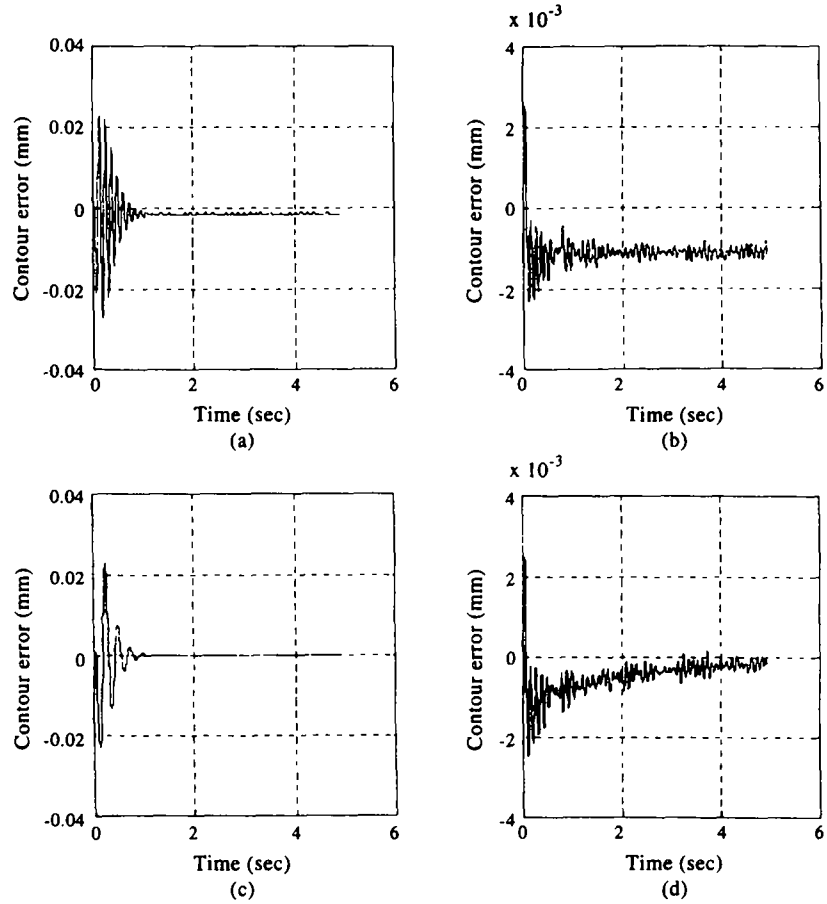


Fig. 5. Figures of simulation result of four schemes for a linear contour: (a) US, (b) CCS, (c) PM, (d) CCPM.

2.3.2. *Simulation results for a circular contour.* At a feedrate $V_b = 11.8$ mm/sec (28 in/min) and radius $R = 30$ mm of the circle, the control gains which issued the best results for the respective methods were also obtained by systematic trial and error, and are tabulated in Tables 3 and 4 (see Fig. 6).

2.3.3. *Discussions for computer simulation.* It is found that the path PM is better for dealing with the elimination of steady-state error for linear contours and the reduction of

Table 3. Gains used for four control schemes for a circular contour

| | $K_v$ | $K_{ex}$ | $K_{ey}$ | $K_{ex}$ | $K_{ey}$ |
|---|---|---|---|---|---|
| US | 0 | 0 | 0 | 1.2 | 1.2 |
| CCS | 0 | 1.5 | 1.5 | 0.8 | 0.8 |
| PM | 7 | 0 | 0 | 0.65 | 0.65 |
| CCPM | 5 | 1 | 1 | 0.8 | 0.8 |

Table 4. Simulation results corresponding to Table 3

| | Fig. 6 | $\lvert\epsilon_{max}\rvert$ ($\mu$m) |
|---|---|---|
| US | (a) | 26 |
| CCS | (b) | 9 |
| PM | (c) | 7 |
| CCPM | (d) | 5 |

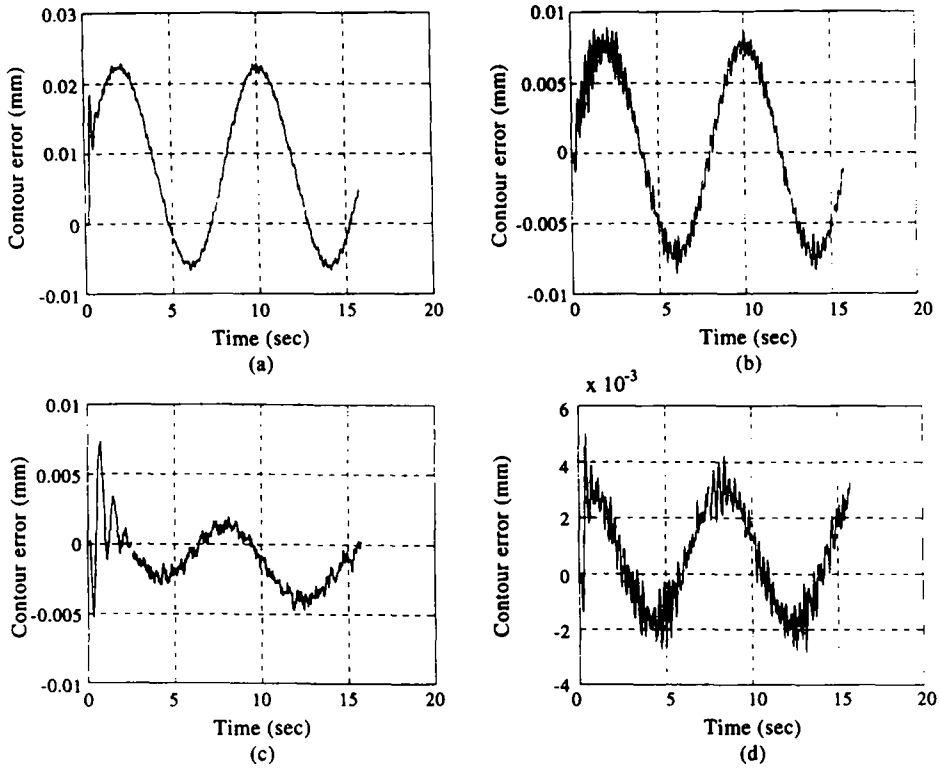


Fig. 6. Figures of simulation result of four schemes for a circular contour: (a) US, (b) CCS, (c) PM, (d) CCPM.

contour error for circular contours than the uncoupled system (US) and conventional CCS. The CCPM, which combines the advantages of CCS and PM, is able to achieve the best accuracy among these control systems on computer simulation for the contour tracking of a CNC machine tool.

## 3. EXPERIMENTAL STUDIES ON THE CROSS-COUPLED PRECOMPENSATION METHOD

### 3.1. *Experimental arrangement*

Figure 7 shows a 600 mm×600 mm $X$–$Y$ table. The $X$- and $Y$-axes of this table include a linear scale of 1 $\mu$m resolution, a linear guideway of 10 mm/rev. lead, a d.c. servomotor and its driver, a power supply and three limit sensors. First, the power supply is used to unlock the brakes of the two d.c. servomotors by supporting 50 V direct current to them. The control signals of the digital-to-analog converter (DAC) for d.c. servomotors and the digital signals of limit sensors are transmitted by an Ax-5411 IO-card. The pulses of digital linear scales are counted by two counter interface ICs HCTL-2016 and transmitted by a 8255 interface card. The number of pulses generated by the linear scale represents position, and the pulse frequency is proportional to the axial velocity. The interface cards are hosted by a 386-PC which also performs all computations and takes control of the experiments.

### 3.2. *Experimental studies for the open-loop system, uncoupled system, cross-coupled control system, precompensation method and cross-coupled precompensation method*

At a representative feedrate of 11.8 mm/sec, which had been reported in [3, 5], the computer simulation results as presented in Section 2.3 of this paper proved that the PM is able to achieve a contour precision better than the CCS proposed in [3, 5]. Furthermore, the CCPM performs well not only in circular contours but also with linear contours. The CCPM offers the highest precision among the US, CCS, PM and CCPM. In this section, the effects of these control schemes will be compared empirically. During the experimental process, $K_{ex} = K_{ey}$ and $K_{ex} = K_{ey}$. Finally, the experimental results are quantified by the "integral absolute error (IAE) criterion" and "integral-of-time-multiplied absolute error (ITAE) criterion". They are defined as follows [11]:

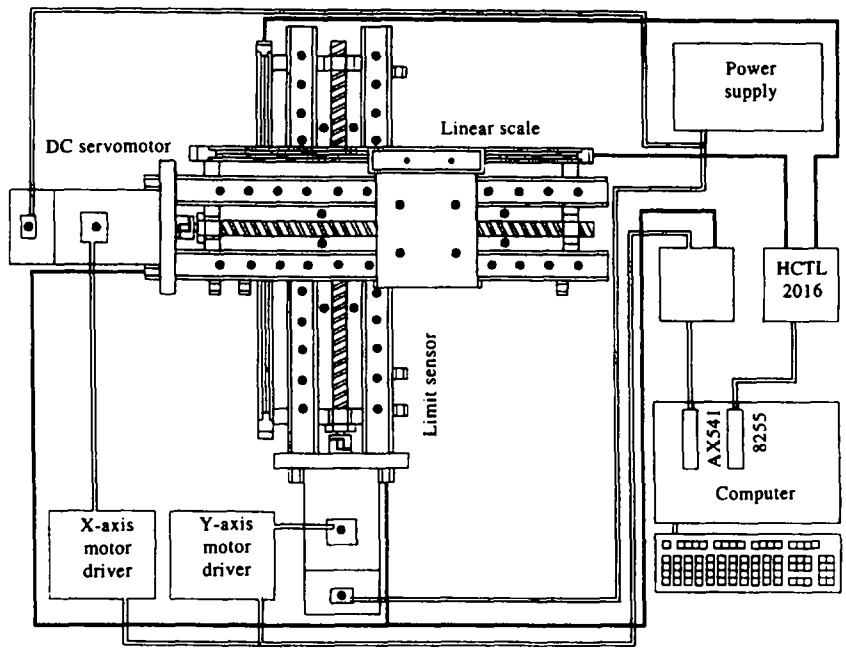


Fig. 7. Top view of the experimental apparatus.

$$\text{IAE: } \frac{1}{N}\sum_{i=1}^{N}|\epsilon(i)|$$

$$\text{ITAE: } \frac{1}{N}\sum_{i=1}^{N}t(i)|\epsilon(i)|.$$

3.2.1. *Linear tracking and selection of gains.* For the trajectory of linear contour, a feedrate of 11.8 mm/sec and $\phi$ of 45° are considered. The experimental sample time was 5 msec and each experimental duration was 20 sec, so the total displacement of the linear trajectory was 221.6 mm. In Fig. 8, the absolute value of the maximum contour errors

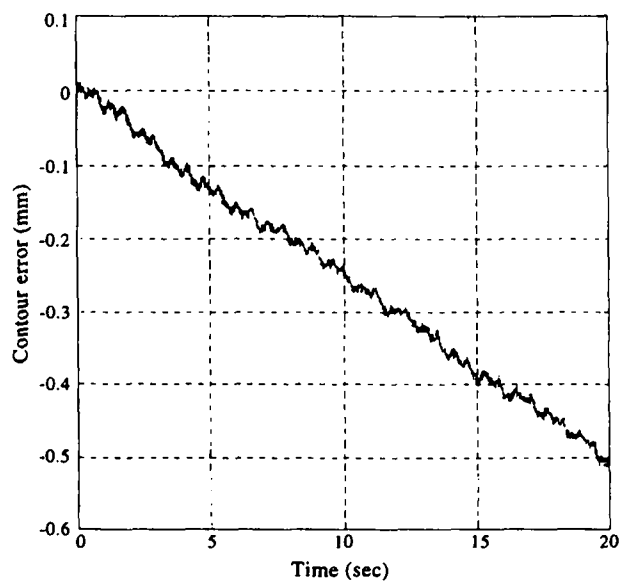


Fig. 8. Experimental result of a linear contour by OS at a feedrate of 11.8 mm/sec.

was about 0.5 mm and the accumulation of contour errors was caused by the nature of open-loop system (OS), which represents $K_v$, $K_{ex}$, $K_{ey}$, $K_{ex}$ and $K_{ey}$ set to zero. Because of this, the contour error would not converge to a constant steady-state error as predicted by computer simulation.

In order to find the gains which yield the smallest contour errors for the respective systems, a systematic trial-and-error procedure was used. At the beginning of the experiment, $K_v$, $K_{ex}$ and $K_{ey}$ were set to zero and $K_{ex}$, $K_{ey}$ were adjusted for US. The values of $K_{ex}$ and $K_{ey}$ were increased from 0.001 at an incremental interval of 0.001, 0.01 or 0.1, but each time with only one effective digit, while the values of $|\epsilon_{max}|$ kept reducing. When the values of $|\epsilon_{max}|$ began to increase, the experiment was halted and the smallest values of $|\epsilon_{max}|$ adopted as the representation for US. As an experimental result, $K_{ex}$ and $K_{ey}$ of 0.01 yield the most precise trajectory for linear contours by US, corresponding to a $|\epsilon_{max}|$ of 395 $\mu$m. With the values 0.01 of $K_{ex}$ and $K_{ey}$ to maintain the tracking precision, the control gains $K_{ex}$ and $K_{ey}$ are added for CCS. The $K_{ex}$ and $K_{ey}$ values were also increased from 0.0001 at incremental intervals of 0.0001, 0.01, 0.1 or 1 before the smallest values of $|\epsilon_{max}|$ appeared. At a group of control gains, $K_{ex}$, $K_{ey}$ being equal to 0.05 and $K_{ex}$, $K_{ey}$ being equal to 0.001, the best contour precision, of 36 $\mu$m, was obtained for CCS. In a similar way, when control gains $K_v$ were equal to 1 and $K_{ex}$, $K_{ey}$ equal to 0.001, the best contour precision of 49 $\mu$m was obtained for PM. Keeping $K_{ex}$ and $K_{ey}$ at 0.01 for the CCPM, the trial-and-error method was used within a range of $K_v$ from 0.01 to 1 and $K_{ex}$, $K_{ey}$ from 0.1 to 10. The most precise contour was 33 $\mu$m by CCPM. Table 5 and Fig. 9 show the comparisons of the individual best experiment results for the US, CCS, PM and CCPM.

3.2.2. *Circular tracking and selection of gains.* For the trajectory of a circular contour, the representative feedrate was still chosen as 11.8 mm/sec, the radius $R$ of the circle was 30 mm and the period $P$ of the circular tracking was 16 sec/rev. In the experimental process, the sample time of the control systems was 5 msec and the total experiment time was 20 sec. The individual velocities are $v_{bx} = 11.8\times\cos((2\pi)/(P)t+1.5\pi)$ and $v_{by} = 11.8\times\sin((2\pi)/(P)t+1.5\pi)$. Following the same experimental method described in Section 3.2.1, the smallest contour errors $|\epsilon_{max}|$ at a feedrate of 11.8 mm/sec were 8275 $\mu$m for US, 93 $\mu$m for CCS, and it could be reduced to 38 $\mu$m by PM. Both computer simulations and experiments confirm that PM and CCS can both improve the precisions of desired trajectories very conspicuously. Specifically, the CCS is better for a linear trajectory and PM is better for a non-linearly circular trajectory at a moderate feedrate. Beyond that, the smallest contour error $|\epsilon_{max}|$ of the proposed CCPM was only 28 $\mu$m at a feedrate of 11.8 mm/sec. This value of $|\epsilon_{max}|$ was far smaller than 8275 $\mu$m for US, 93 $\mu$m for CCS and 38 $\mu$m for PM. Figure 10 shows the experimental results for the OS. Table 6(a), (b)

Table 5. Experimental results for linear contour at a feedrate of 11.8 mm/sec

(a) Control gains for four control schemes

| | $K_v$ | $K_{ex}$ | $K_{ey}$ | $K_{ex}$ | $K_{ey}$ |
|---|---|---|---|---|---|
| US | 0 | 0 | 0 | 0.01 | 0.01 |
| CCS | 0 | 0.05 | 0.05 | 0.01 | 0.01 |
| PM | 1 | 0 | 0 | 0.01 | 0.01 |
| CCPM | 0.2 | 0.07 | 0.07 | 0.01 | 0.01 |

(b) Experimental results

| | Fig. 9 | $\lvert\epsilon_{max}\rvert$ ($\mu$m) | IAE | ITAE |
|---|---|---|---|---|
| US | (a) | 395 | 174.5064 | 2.3661 |
| CCS | (b) | 36 | 12.5402 | 0.1310 |
| PM | (c) | 49 | 16.0371 | 0.1654 |
| CCPM | (d) | 33 | 11.0311 | 0.1199 |

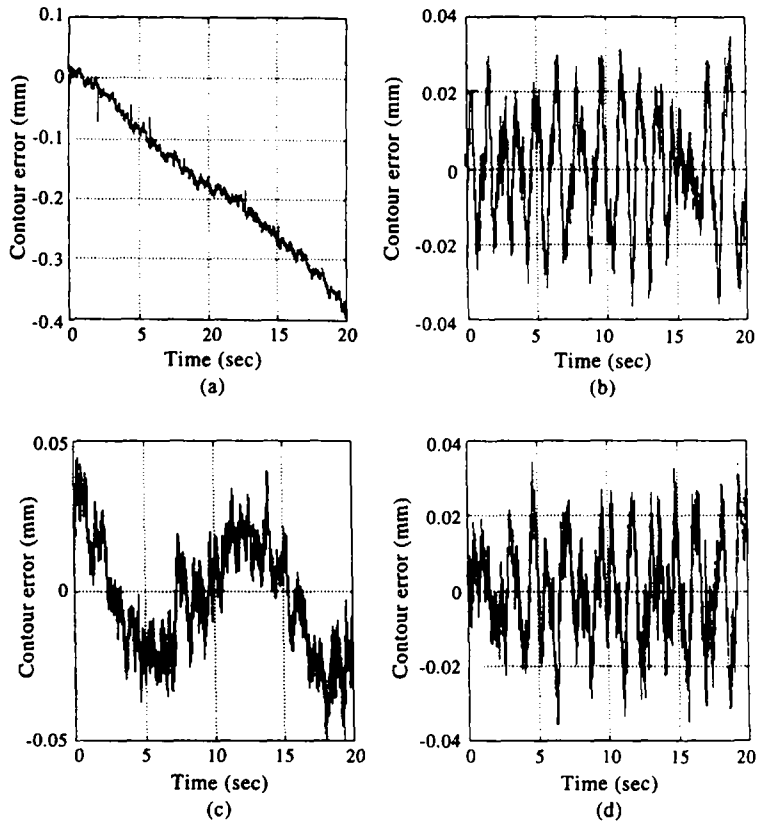


Fig. 9. Experimental comparisons for a linear contour at a feedrate of 11.8 mm/sec: (a) US, (b) CCS, (c) PU, (d) CCPM.

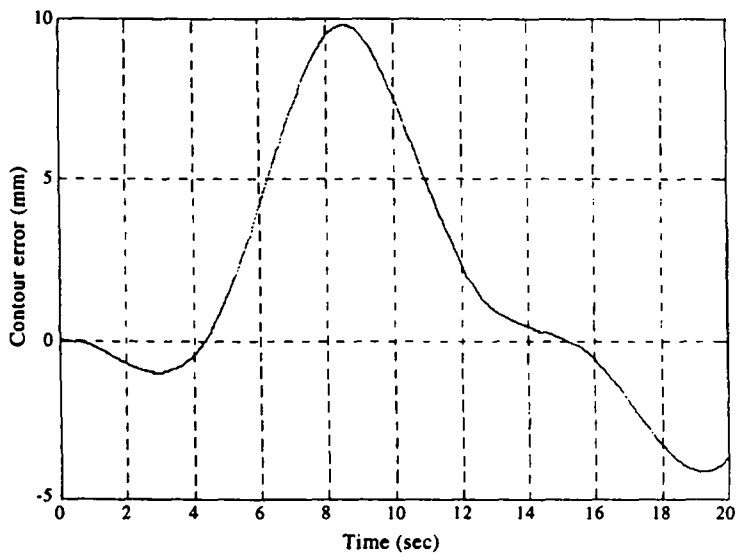


Fig. 10. Contour errors of a circular contour by OS at a feedrate of 11.8 mm/sec.

and Fig. 11 were the comparisons of individually best experimental results for US, CCS, PM and CCPM.

### 3.3. *Experimental studies on high feedrate*

For the multi-axis machine tool, high spindle speeds require a high feedrate for appropriate machining. Srinivasam [4] has investigated the CCS at higher feedrates, varying from 37.5 mm/sec to 120 mm/sec. In this study, a linear leadscrew of 10 mm/rev is used to

Table 6. Experimental results for a circular contour at a feedrate of 11.8 mm/sec

(a) Control gains for four control schemes

| | $K_v$ | $K_{ax}$ | $K_{cy}$ | $K_{ex}$ | $K_{ey}$ |
|---|---|---|---|---|---|
| US | 0 | 0 | 0 | 0.01 | 0.01 |
| CCS | 0 | 0.1 | 0.1 | 0.01 | 0.01 |
| PM | 0.01 | 0 | 0 | 0.01 | 0.01 |
| CCPM | 0.007 | 0.03 | 0.03 | 0.01 | 0.01 |

(b) Experimental results

| | Fig. 11 | $\lvert\epsilon_{max}\rvert$ ($\mu$m) | IAE×10$^3$ | ITAE×10$^4$ |
|---|---|---|---|---|
| US | (a) | 8275 | 3.5804 | 4.1003 |
| CCS | (b) | 93 | 0.0325 | 0.0461 |
| PM | (c) | 38 | 0.0085 | 0.0083 |
| CCPM | (d) | 28 | 0.0066 | 0.0064 |

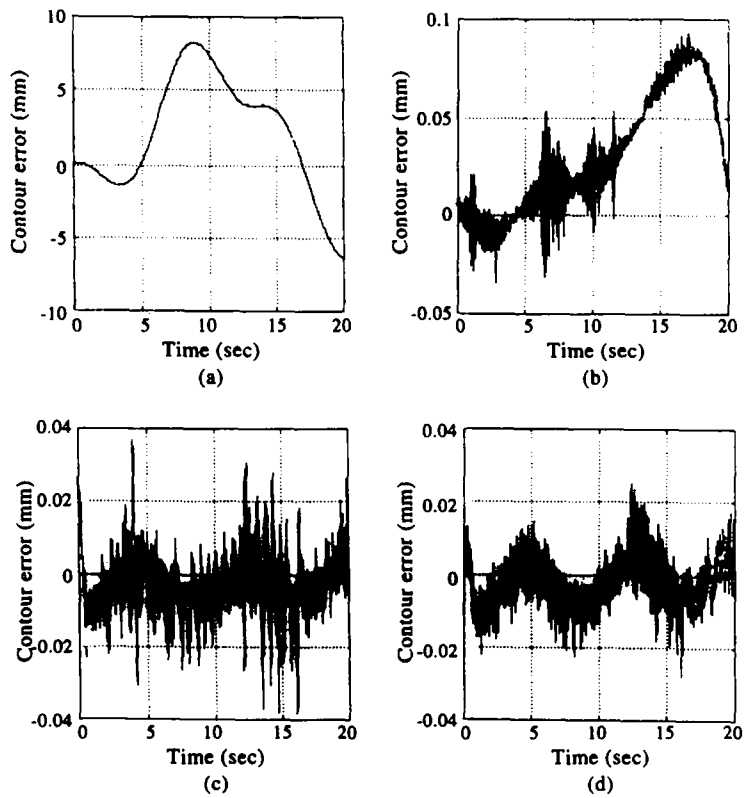


Fig. 11. Experimental comparisons for a circular contour at a feedrate of 11.8 mm/sec: (a) US, (b) CCS, (c) PM, (d) CCPM.

achieve the high feedrate varying from 50 to 200 mm/sec, and a linear scale of 1 $\mu$m resolution is used to measure the direct position. The sample time for the control system is 5 msec and the total experimental duration is 2 sec for linear trajectories at any feedrates, and 4 sec for radii of the circular contour of 30, 60, 90, 120 mm at feedrates of 50, 100, 150, 200 mm/sec, respectively.

3.3.1. *Linear tracking.* At the inclined angle $\phi = 45°$ of the desired linear relative contour to the $X$-axis, following a similar trial-and-error method to that decribed in Section

3.2.1, Table 7 and Fig. 12 show the experimental results of the linear trajectory at the feedrate of 50 mm/sec. Table 8 and Fig. 13 indicate the experimental results of the linear trajectory at the feedrate of 100 mm/sec. Table 9 and Fig. 14 show the experimental results of the linear trajectory at the feedrate of 150 mm/sec. Table 10 and Fig. 15 show the experimental results of the linear trajectory at the feedrate of 200 mm/sec.

3.3.2. *Circular tracking.* The results obtained using a similar experimental method to that described in Section 3.2.1 are shown in Table 11 and Fig. 16. Table 12 and Fig. 17 show the experimental results of a full circle with a radius of 60 mm at the feedrate of 100 mm/sec. Table 13 and Fig. 18 show the experimental results of circular trajectory at the feedrate of 150 mm/sec. Table 14 and Fig. 19 show the experimental results of a circular trajectory at the feedrate of 200 mm/sec.

Table 7. Experimental results for a linear contour at a feedrate of 50 mm/sec

| | Fig. 12 | $\lvert\epsilon_{max}\rvert$ ($\mu$m) | IAE | ITAE |
|---|---|---|---|---|
| US | (a) | 114 | 109.8773 | 146.5803 |
| CCS | (b) | 37 | 11.2214 | 10.2573 |
| PM | (c) | 40 | 10.9460 | 10.0071 |
| CCPM | (d) | 36 | 11.3664 | 11.1544 |

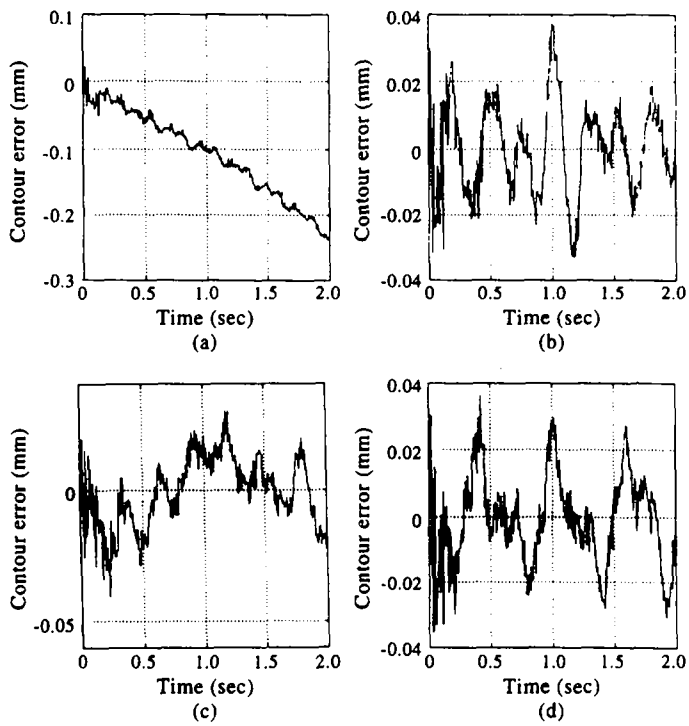


Fig. 12. Experimental comparisons for a linear contour at a feedrate of 50 mm/sec: (a) US, (b) CCS, (c) PM, (d) CCPM.

Table 8. Experimental results for a linear contour at a feedrate of 100 mm/sec

| | Fig. 13 | $\lvert\epsilon_{max}\rvert$ ($\mu$m) | IAE | ITAE |
|---|---|---|---|---|
| US | (a) | 826 | 409.6849 | 554.2313 |
| CCS | (b) | 60 | 23.8775 | 23.2669 |
| PM | (c) | 77 | 29.3676 | 30.3675 |
| CCPM | (d) | 56 | 22.7510 | 22.8326 |

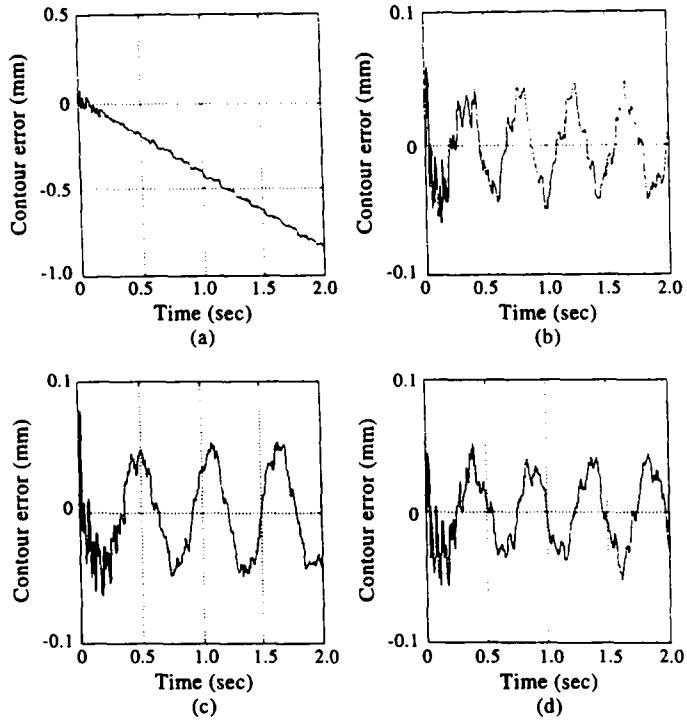


Fig. 13. Experimental comparisons for a linear contour at a feedrate of 100 mm/sec: (a) US, (b) CCS, (c) PM, (d) CCPM.

Table 9. Experimental results for linear contour at a feedrate of 150 mm/sec

| | Fig. 14 | $\lvert\epsilon_{max}\rvert$ ($\mu$m) | IAE | ITAE |
|---|---|---|---|---|
| US | (a) | 1241 | 586.8913 | 805.2127 |
| CCS | (b) | 86 | 39.6578 | 39.7439 |
| PM | (c) | 106 | 55.2789 | 55.7948 |
| CCPM | (d) | 78 | 36.3815 | 37.3844 |

### 3.4. *Discussions of experiment*

3.4.1. *Path precompensation method for tracking.* Experimental results, as recorded in Table 5, Table 6, Fig. 9(a), (b), (c), Fig. 11(a), (b), (c) or redrawn in Fig. 20, Fig. 21, show that the PM scheme is comparable to the CCS scheme in linear contour, but to some extent better than the CCS scheme in circular contour, as shown in Fig. 22. For instance, Table 6 had shown that the best experimental results of US, CCS and PM about the contour error $|\epsilon_{max}|$ were 8275 $\mu$m, 93 $\mu$m and 38 $\mu$m, respectively. Furthermore, the performance indexes of IAE/ITAE were 3.5804/4.1003 for US, 0.0325/0.0461 for CCS, and 0.0085/0.0083 for PM. These two indexes of IAE and ITAE refer to the magnitude of error with different emphasis: the smaller they appear, the better they are. To sum up, PM has the better performance with about 1.4 times less contour error $|\epsilon_{max}|$, 2.8 times less IAE and 4.6 times less ITAE than CCS. It is seen that the PM is a better control scheme than CCS in dealing with the circular contour.

3.4.2. *Cross-coupled precompensation method.* For a linear tracking at a feedrate of 11.8 mm/sec, Table 5 and Fig. 9 show that the CCPM achieved the smallest values of not only the contour error $|\epsilon_{max}|$ 33 $\mu$m, but also IAE and ITAE values of 11.0311 and 0.1199. By comparing the effect of CCS and CCPM, we discover that the CCPM has the better performance with about 8% less contour error $|\epsilon_{max}|$, 12% less for the IAE index and 8% less for the ITAE index. Also, the CCPM is about 33% less than the contour error $|\epsilon_{max}|$, 30% less for IAE and 28% for the ITAE than PM.

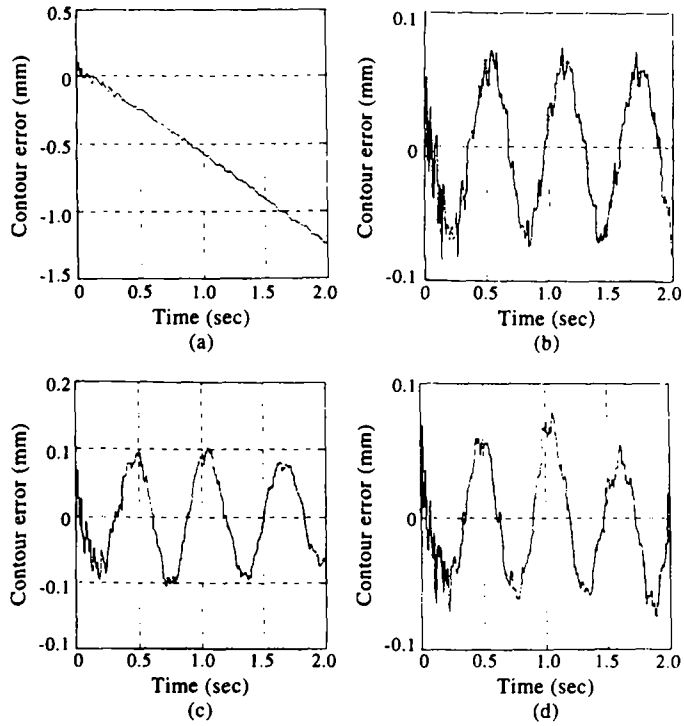


Fig. 14. Experimental comparisons for a linear contour at a feedrate of 150 mm/sec: (a) US, (b) CCS, (c) PM, (d) CCPM.

Table 10. Experimental results for a linear contour at a feedrate of 200 mm/sec

| | Fig. 15 | $\lvert\epsilon_{max}\rvert$ ($\mu$m) | IAE | ITAE$\times 10^4$ |
|---|---|---|---|---|
| US | (a) | 1576 | 749.5903 | 1.0254 |
| CCS | (b) | 155 | 85.4016 | 0.0855 |
| PM | (c) | 166 | 65.1590 | 0.0545 |
| CCPM | (d) | 135 | 74.9417 | 0.0777 |

From the results of Table 6 or Fig. 11, the CCPM is also much more effective in increasing the contour precision of circular contours than CCS. For instance, the contour error $|\epsilon_{max}|$ could be reduced from 93 $\mu$m to 28 $\mu$m, and the index of IAE was from 0.0325 to 0.0066 and the ITAE was from 0.0461 to 0.0064. Experiments show that the CCPM was the best one among US, CCS, PM, and CCPM for any high precision trajectories at a representative feedrate of 11.8 mm/sec.

3.4.3. *Precompensation method and cross-coupled precompensation method at high feedrate.* From the experimental results for circular trajectories shown in Fig. 17(b), Fig. 18(b) and Fig. 19(b), if the feedrates are higher than 50 mm/sec, the CCS will fail to converge. The contour error $|\epsilon_{max}|$ and the contour becomes a spiral toward the center of the circle, while the PM and CCPM can still be maintained. The advantages of PM and CCPM become more obvious at higher feedrates, especially the CCPM as shown in Table 15 and Figs 23 and 24. The obvious increase in the ratio $|\epsilon_{max}|_{CCS}/|\epsilon_{max}|_{CCPM}$ indicates that the CCPM is more effective than CCS in obtaining a precise trajectory at an elevated feedrate.

## 4. CONCLUSION

The concept and computer simulations of the path PM for robotic trackings are proposed by Chin and Tsai [9], and the CCS [2–5] has been successful since 1980 in reducing the contour error of desired trajectories at moderate feedrates, such as 11.8 and 20 mm/sec,

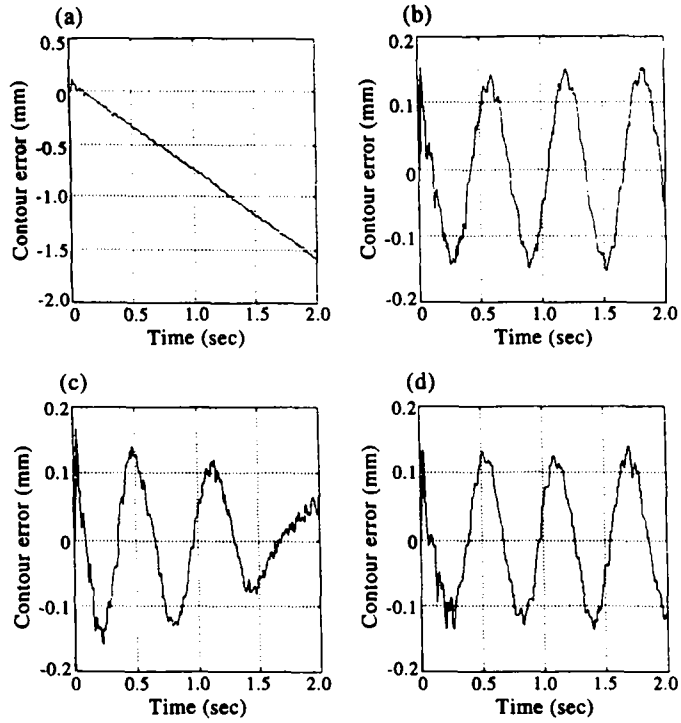


Fig. 15. Experimental comparisons for a linear contour at a feedrate of 200 mm/sec: (a) US, (b) CCS, (c) PM, (d) CCPM.

Table 11. Experimental results for a circular contour of radius 30 mm at a feedrate of 50 mm/sec

| | Fig. 16 | $\lvert\epsilon_{max}\rvert$ ($\mu$m) | IAE×10³ | ITAE×10³ |
|---|---|---|---|---|
| US | (a) | 3180 | 1.1253 | 2.0975 |
| CCS | (b) | 54 | 0.0118 | 0.0265 |
| PM | (c) | 50 | 0.0190 | 0.0360 |
| CCPM | (d) | 40 | 0.0125 | 0.0232 |

Table 12. Experimental results for a circular contour of radius 60 mm at a feedrate of 100 mm/sec

| | Fig. 17 | $\lvert\epsilon_{max}\rvert$ ($\mu$m) | IAE×10³ | ITAE×10³ |
|---|---|---|---|---|
| US | (a) | 2629 | 1.6538 | 3.8790 |
| CCS | (b) | 110 | 0.0400 | 0.1038 |
| PM | (c) | 92 | 0.0337 | 0.0657 |
| CCPM | (d) | 60 | 0.0187 | 0.0378 |

etc. In this study, we propose a CCPM with the intention of combining the advantages of the PM and CCS, for a CNC machine tool. This CCPM is tested by computer simulation, experimentally tested and compared with the US, CCS and PM. The study also provides experimental confirmation that the PM is better than the US and CCS in the elimination of steady-state errors for linear contours and in reducing contour errors for circular contours. Experimental results show that the CCS is better for linear trajectories and the PM is better for circular trajectory.

Most of all, computer simulations and experimental results prove that the CCPM is better than the US, CCS and PM in dealing with not only the elimination of steady-state errors for linear contours but also in the reduction of contour errors for linear and circular contours.

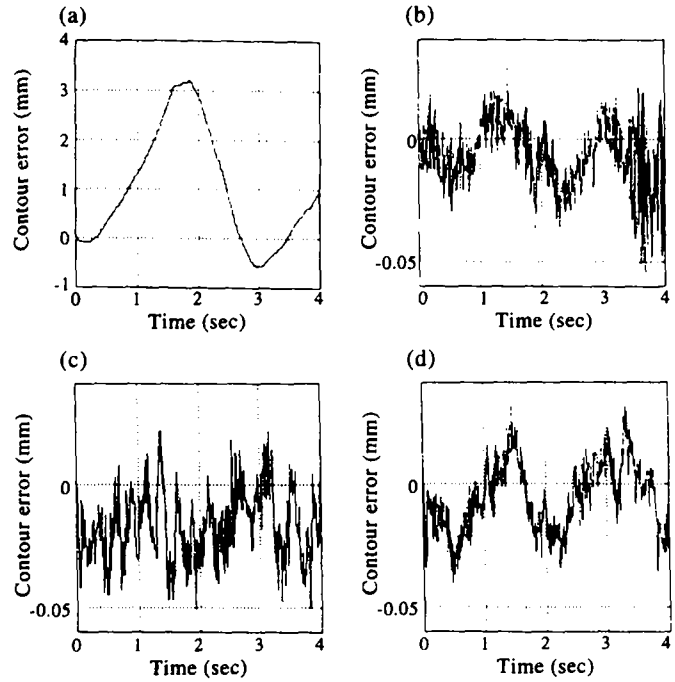


Fig. 16. Experimental comparisons for a circular contour at a feedrate of 50 mm/sec: (a) US, (b) CCS, (c) PM, (d) CCPM.

Table 13. Experimental results for a circular contour of radius 90 mm at a feedrate of 150 mm/sec

| | Fig. 18 | $\lvert\epsilon_{max}\rvert$ ($\mu$m) | IAE×10$^3$ | ITAE×10$^3$ |
|---|---|---|---|---|
| US | (a) | 5738 | 2.5431 | 5.9749 |
| CCS | (b) | 490 | 0.1995 | 0.5448 |
| PM | (c) | 259 | 0.0619 | 0.1340 |
| CCPM | (d) | 117 | 0.0295 | 0.0701 |

Table 14. Experimental results for a circular contour of radius 120 mm at a feedrate of 200 mm/sec

| | Fig. 19 | $\lvert\epsilon_{max}\rvert$ ($\mu$m) | IAE×10$^3$ | ITAE×10$^3$ |
|---|---|---|---|---|
| US | (a) | 7293 | 3.1352 | 6.3319 |
| CCS | (b) | 701 | 0.2294 | 0.6622 |
| PM | (c) | 420 | 0.1474 | 0.3164 |
| CCPM | (d) | 80 | 0.0302 | 0.0572 |

Table 15. Experimental comparison at different feedrates

| Feedrate (mm/sec) | $(\lvert\epsilon_{max}\rvert_{CCS})/(\lvert\epsilon_{max}\rvert_{CCPM})$ | $(IEA_{CCS})/(IEA_{CCPM})$ | $(ITEA_{CCS})/(ITEA_{CCPM})$ |
|---|---|---|---|
| 50 | 1.35 | 0.94 | 1.14 |
| 100 | 1.83 | 2.14 | 2.74 |
| 150 | 4.19 | 6.76 | 7.77 |
| 200 | 8.76 | 7.60 | 11.58 |

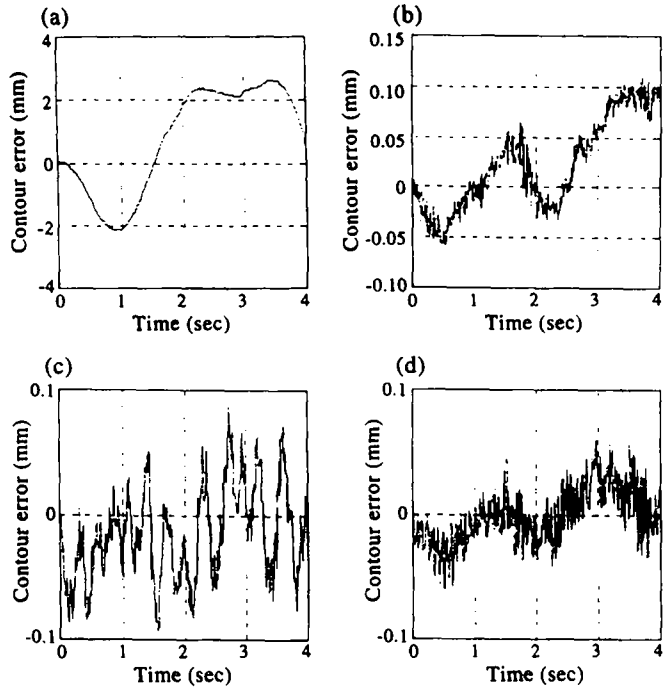


Fig. 17. Experimental comparisons for a circular contour at a feedrate of 100 mm/sec: (a) US, (b) CCS, (c) PM, (d) CCPM.

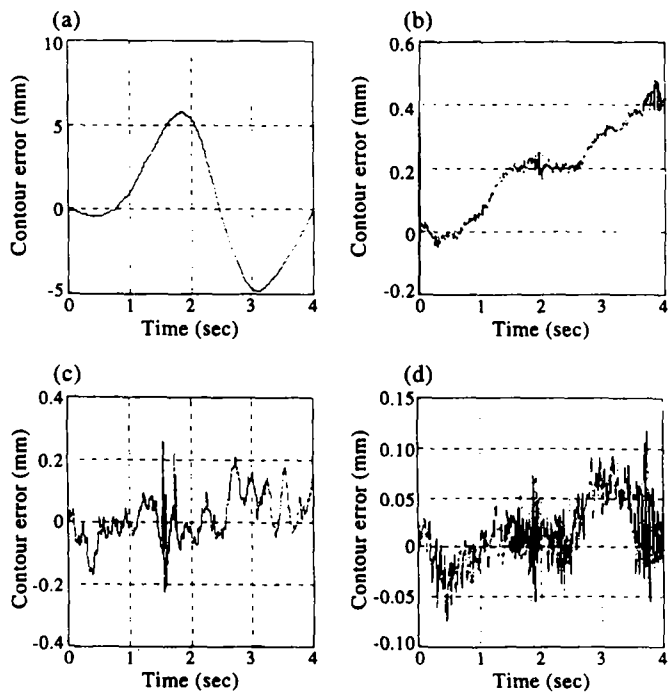


Fig. 18. Experimental comparisons for a circular contour at a feedrate of 150 mm/sec: (a) US, (b) CCS, (c) PM, (d) CCPM.

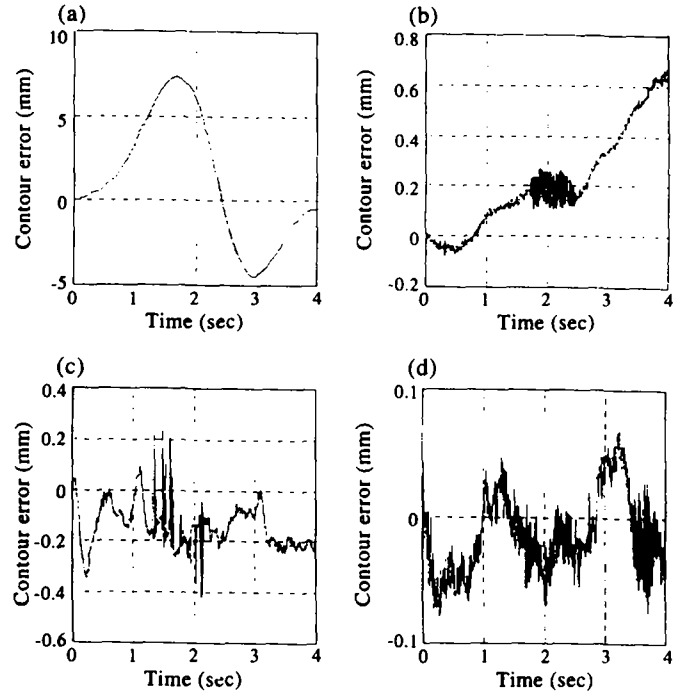


Fig. 19. Experimental comparisons for a circular contour at a feedrate of 200 mm/sec: (a) US, (b) CCS, (c) PM, (d) CCPM.

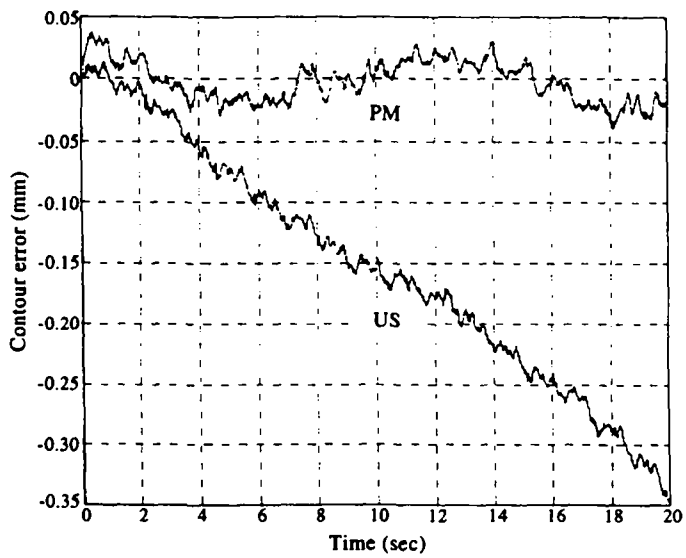


Fig. 20. Empirical comparison of US and PM for a linear contour at a feedrate of 11.8 mm/sec.

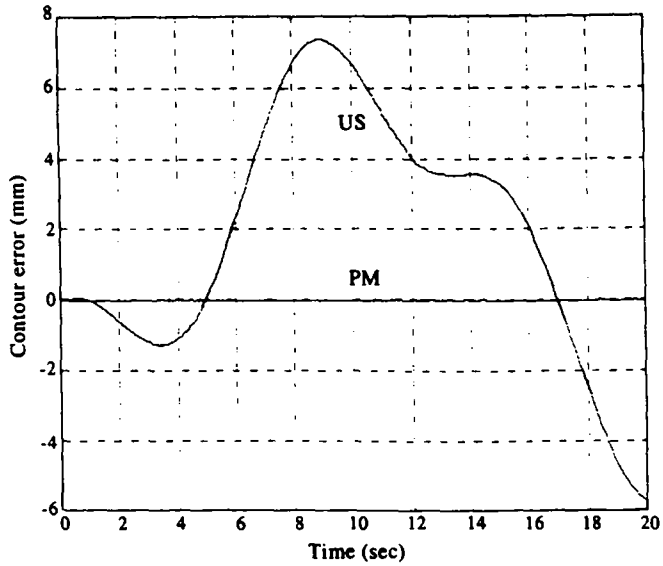


Fig. 21. Empirical comparison of US and PM for a circular contour at a feedrate of 11.8 mm/sec.

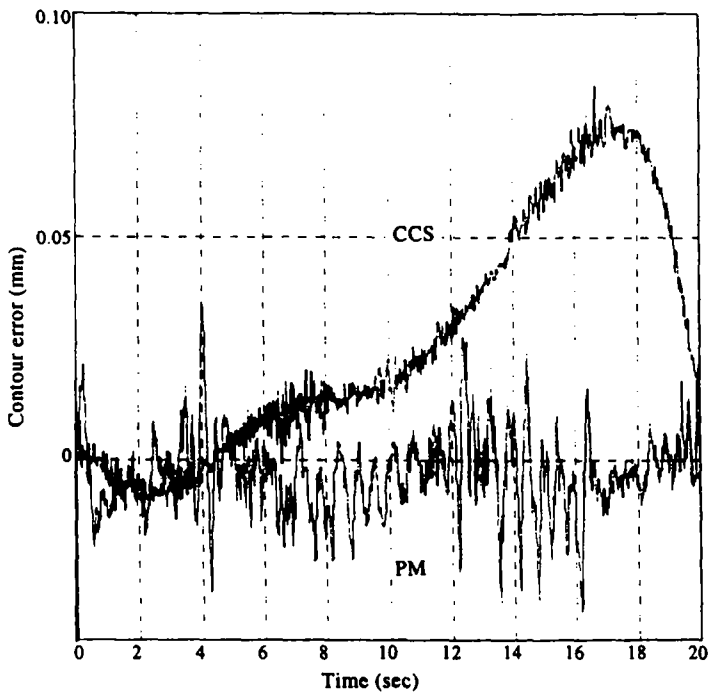


Fig. 22. Empirical comparisons of PM and CCS at a feedrate of 11.8 mm/sec for a a circular contour.

The experimental results indicate that, at a feedrate higher than 50 mm/sec, for circular trajectories the conventional CCS will fail to converge the values of the contour errors, which leads to a spiral trajectory toward the center of the circle. This problem can be effectively solved by the CCPM. Furthermore, the advantages of the PM and CCPM, especially the CCPM, are enhanced at higher feedrates. At a feedrate of 200 mm/sec the CCPM is significantly better.

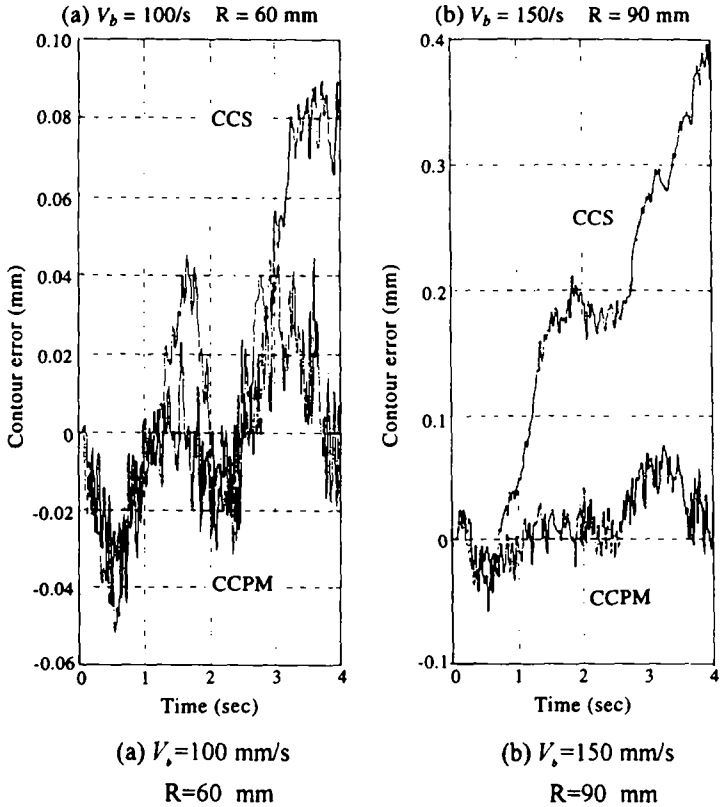


Fig. 23. Empirical comparisons of CCS and PM for a circular contour at different feedrates.

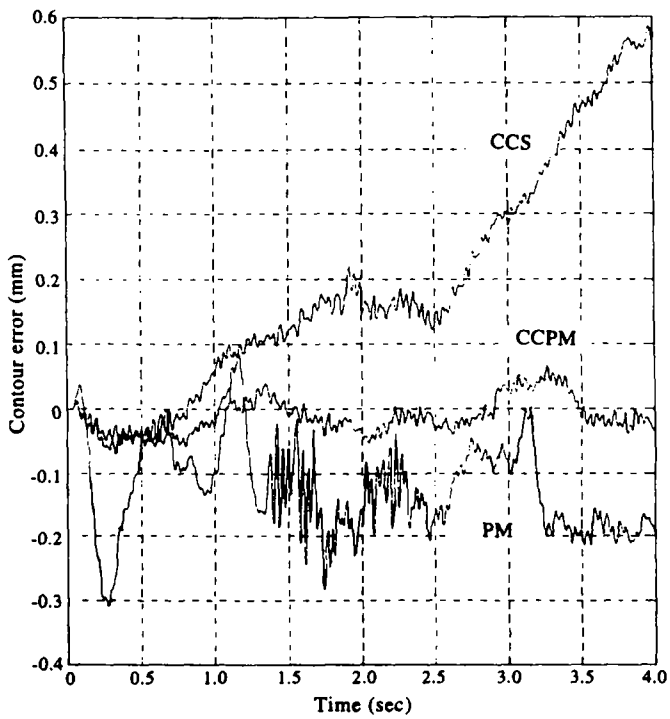


Fig. 24. Empirical comparisons for a circular contour ($R$ = 120 mm) at a feedrate of 200 mm/sec

*Acknowledgements*—This research was supported by the National Science Council of the Republic of China under Grant No. NSC-82-0422-E-009-330.

## REFERENCES

[1] P. Sarachik and J.R. Ragazzini, A two dimensional feedback control system, *Transactions of the AIEE* **76**, 55–61 (1957).
[2] Y. Koren and J. Ben-Uri, Digital control of multi-axial motion system, *IFAC 5th Word Congress, Paris, Proceedings*, Vol. 1, Section II, 1972.
[3] Y. Koren, Cross-coupled biaxial computer control for manufacturing, *ASME Transactions, Journal of Dynamic Systems, Measurement and Control* **201**, 265–272 (1980).
[4] P.K. Kulkami and K. Srinivasan, Cross-coupled control of biaxial feed drive servomechanisms, *ASME Transactions, Journal of Dynamic Systems, Measurement and Control* **112**, 225–232 (1990).
[5] Y. Koren and C.-C. Lo, Variable-gain cross-coupling controller for contouring, *Annals of CIRP* **40**, 371–374 (1991).
[6] H.-Y. Chuang and C.-H. Liu, Cross-coupled adaptive feedrate control for multiaxis machine tools, *ASME Transactions, Journal of Dynamic Systems, Measurement and Control* **113**, 451–457 (1991).
[7] H.-Y. Chuang and C.-H. Liu, A model-referenced adaptive control strategy for improving contour accuracy of multi-axis machine tools, *IEEE Transactions on Industrial Application* **28**, 221–227 (1992).
[8] S.-J. Huang and C.-C. Chen, Application of self-tuning feed-forward and crosscoupling control in a retrofitted milling machine, *International Journal of Machine Tools & Manufacture* **35**, 577–591 (1995).
[9] J.-H. Chin and H.-C. Tsai, A path algorithm for robotics machining, *Robotics & Computer-Integrated Manufacturing* **10**, 185–198 (1993).
[10] J. Huan, Bahnregelung zur Bahnerzeugung an numerisch gesteuerten Werkzeugmaschinen. Dissertation, University of Stuttgart, 1982.
[11] K. Ogata, *Modern Control Engineering*. Prentice-Hall, Englewood Cliffs, NJ, 1990.